

Comparative Botanical and Phytochemical Studies of Ambiguous Medicinal Plant Species of *Wedelia* and *Eclipta* (Fam. Asteraceae) Used in ASU Systems of Medicine with Special Reference to *in-silico* Screening of Hepatoprotective Potential of Marker Wedelolactone with Acetaminophen Targets

C. Arunachalam, R. Arunadevi¹, S. Murugammal², N. Monika¹, R. Susila³, S. N. Sunil Kumar⁴

Departments of Botany and ¹Pharmacology, Captain Srinivasa Murthy Regional Ayurveda Drug Development Institute, (CCRAS, Ministry of AYUSH, Government of India, New Delhi), Anna Hospital Campus, Departments of ²Chemistry, ³Clinical Research and ⁴Botany, Siddha Central Research Institute, (CCRS, Ministry of AYUSH, Government of India, Chennai), Anna Hospital Campus, Chennai, Tamil Nadu, India

ABSTRACT

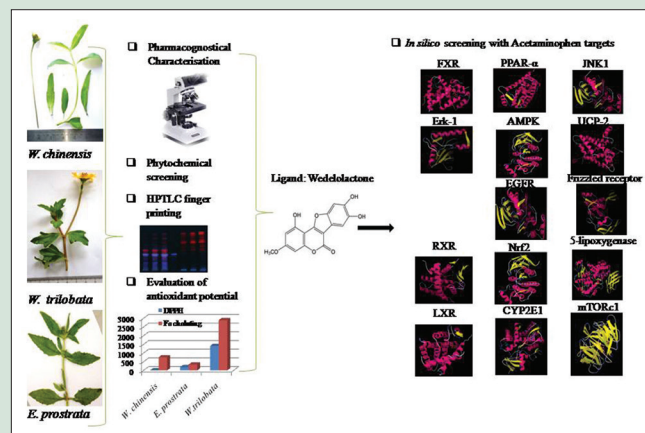
Context: In traditional medicine, *Kesaraja* (Ayurveda) or *Manjal karisali* (Siddha) is effective for jaundice. **Aim:** Three species of Asteraceae need to be studied for their therapeutic superiority of their intended claim. They are *Wedelia chinensis* (Osbeck) Merr. Philipp J., *Wedelia trilobata* (L.) Hitchc. and *Eclipta prostrata* (L.) L. (Asteraceae). The present study aimed to screen and characterize the potential species for therapeutic purpose. **Materials and Methods:** The whole plants, *W. chinensis* (Osbeck) Merr. Philipp J., *W. trilobata* (L.) Hitchc. and *Eclipta prostrata* (L.) (Asteraceae) were collected and botanically identified. Preliminary phytochemical analysis and high-performance thin-layer chromatography finger printing with marker wedelolactone were done for the ethanolic extracts of these plants. Botanical and pharmacognostical diagnostic characters of the plants based on macro-morphological, micro-morphological and powder microscopical characterization were worked out. Comparative *in-vitro* antioxidant potential of ethanolic extracts of these plant species was carried out. Using ADMET SAR software, the pharmacokinetics of wedelolactone were predicted. Using Autodock 4.2 software, the binding energy of wedelolactone on targets of acetaminophen-induced hepatotoxicity namely PPAR- α , AMPK, JNK-1, EGFR, Nrf2, ALT, ALP, GGT, CAR, Frizzled receptor, FXR, ERK1, LXR, mitochondrial glutamate dehydrogenase, p53, mTOR C1, CYP1A2, CYP2E1, 5-lipoxygenase, thrombin, UCP1, GSK1, RXR and PXR was predicted. **Results:** All the three plant species were pharmacognostically and chemically different. *W. chinensis* was found to possess more antioxidant potential than the other two plants. The marker compound wedelolactone was not detected in *W. trilobata*. Wedelolactone confirmed high binding affinity toward PPAR- α , AMPK, Nrf2, CYP2E1, EGFR, JNK1, UCP-2, thrombin, 5-lipoxygenase, mTORC1, RXR, FXR, LXR, Frizzled receptor, GDH and Erk-1. **Conclusion:** Based on the above observations, we conclude that the presence of marker compound wedelolactone might have attributed the potency of *W. chinensis* and *E. prostrata* in counteracting acetaminophen toxicity when compared with *W. trilobata*.

Key words: Antioxidant, Ayurveda, Siddha, botany, docking, *Wedelia chinensis*, *Wedelia trilobata*, *Eclipta prostrata*, wedelolactone, high-performance thin-layer chromatography, macro-morphological, micro-morphological, phytochemical, powder microscopy

SUMMARY

• In traditional medicine, *Kesaraja* (Ayurveda) or *Manjal karisali* (Siddha) is

effective for jaundice. Three species of Asteraceae need to be studied for their therapeutic superiority of their intended claim. They are *Wedelia chinensis* (Osbeck) Merr. Philipp J., *Wedelia trilobata* (L.) Hitchc. and *Eclipta prostrata* (L.) L. (Asteraceae). The present study aimed to screen and characterize the potential species for therapeutic purpose with special reference to their antioxidant activity and *in silico* screening of marker wedelolactone with acetaminophen targets. Based on this study, it is concluded that all the three plants are different. *W. trilobata* did not have the marker compound wedelolactone. *In silico* prediction supports the drug likeness of wedelolactone and its interaction with target proteins. The chemical profiling of *W. chinensis* is different from that of *Eclipta prostrata*, but the marker compound is common for both. Because *W. chinensis* and *E. prostrata* were interchangeably used for common ailments, the marker compound wedelolactone might have been responsible for their shared efficacy. *W. chinensis* was observed to be more potent antioxidant than the other two species. Hence, *Wedelia chinensis* may be a potential species for counteracting acetaminophen toxicity either as a drug or as a supportive therapy.



Abbreviations Used: AAP: Acetaminophen; HPTLC: High-performance thin-layer chromatography; ROS: Reactive oxygen species; NAPQI: N-acetyl-p-benzoquinone imine; ER: Endoplasmic reticulum; PPAR α : Peroxisome proliferator activated receptor α ; AMPK: AMP-activated kinase; JNK-1: c-Jun N-terminal Kinase-1; EGFR: Epidermal growth factor

Cite this article as: Arunachalam C, Arunadevi R, Murugammal S, Monika N, Susila R, Kumar SN. Comparative botanical and phytochemical studies of ambiguous medicinal plant species of *Wedelia* and *Eclipta*(Fam. Asteraceae) used in ASU systems of medicine with special reference to *in-silico* screening of hepatoprotective potential of marker wedelolactone with acetaminophen targets. Phcog Res 2020;12:285-98.

Submitted: 15-Feb-2020

Revised: 09-Apr-2020

Accepted: 29-Apr-2020

Published: 14-Aug-2020

This is an open access journal, and articles are distributed under the terms of the Creative Commons Attribution-NonCommercial-ShareAlike 4.0 License, which allows others to remix, tweak, and build upon the work non-commercially, as long as appropriate credit is given and the new creations are licensed under the identical terms.

For reprints contact: reprints@medknow.com

receptor; Nrf2: Nuclear factor erythroid 2-related factor 2; ALT: Alanine transaminase; ALP: Alkaline Phosphatase; GGT: Gamma glutamyl transpeptidase; CAR: Cartesenoide activated receptor; FXR: Farnesoid X Receptor; ERK1: Extracellular signal regulated kinase; LXR: Liver X Receptor-alpha; GDH: Mitochondrial Glutamate dehydrogenase; mTORC1: Mammalian target of Rapamycin Complex; CYP1A2: Cytochrome P450 1A2; CYP2E1: Cytochrome P450 2E1; 5-LO: 5-lipoxygenase; UCP-2: Uncoupling protein 2; GSK-1: Glycogen synthase kinase; RXR: Retinoid X receptor; NF- κ B: Nuclear factor-kappa B; PXR: Pregnane X receptor; UV: Ultraviolet; *W. chinensis*: *Wedelia chinensis*; *W. trilobata*: *Wedelia trilobata*; *E. prostrata*: *Eclipta prostrata*; DPPH: Diphenyl picrazyl hydrazide; IC₅₀: 50% inhibitory concentration; Ro5: Rule of five; ADMET: Absorption, Distribution, Metabolism, Excretion, Toxicity; HIA: Human intestinal absorption; CYP: Cytochrome P; EDTA: Ethylenediaminetetraacetic acid; Log P: Logarithmic value of partition coefficient; Log S: Logarithmic value

of Solubility; H bond: Hydrogen bond; PSA: Polar surface area; BBB: Blood-brain barrier; Ames test: Mutagen identified via toxicity test; FHMT: Fish toxicity; TPT: Tetrahymena pyriformis toxicity; HBT: Honey bee toxicity; GST: Glutathione transferase; GSH: Glutathione; SULF2: Sulfo transferase; GDH: Glutamate dehydrogenase.

Correspondence:

Dr. R. Arunadevi,
Captain Srinivasa Murthy Regional
Ayurveda Drug Development Institute,
(CCRAS, Ministry of AYUSH,
Government of India, New Delhi),
Anna Hospital Campus, Arumbakkam,
Chennai, Tamil Nadu, India.
E-mail: 30aruna@gmail.com
DOI: 10.4103/pr.pr_11_20

Access this article online

Website: www.phcogres.com

Quick Response Code:



INTRODUCTION

The perennial herbs *Wedelia chinensis* (Osbeck) Merr. Philipp J., *Wedelia trilobata* (L.) Hitchc. and *Eclipta prostrata* (L.) L. belong to the family Asteraceae (formerly Compositae).^[1] A decade ago, *W. chinensis* was often used as a substitute for *E. prostrata* due to the confusion in their common name. *W. chinensis* and *W. trilobata* were confused nowadays due to the similarity in their morphology. Being edible in the form of greens, there is a problem in right identification of the species which were misunderstood with one another. Generally, these plants are distributed all over India, mostly in rainy season and all the year around in wet and watery places. There are three different varieties of Bhringraja in the Nighantus, namely, white, black, and yellow. The white is *Eclipta alba* or *E. prostrata*, also named Karicalai in Siddha Formulary of India, and the yellow varieties are *W. chinensis* and *W. trilobata*, whereas the black types of Bhringraja seems to be a variety of *Eclipta* with dark-colored stems.^[2] Because the right medicine for the right ailment is a fundamental requirement in herbal medicine, the current investigation was aimed at comparing these three species pharmacognostically, phytochemically, and *in silico* pharmacologically.

E. prostrata is used as liver tonic and hair growth promoter traditionally in the Indian Systems of Medicine. It is also used in the treatment of spleen enlargements, uterine hemorrhages, skin diseases, and respiratory disorders.^[3] The plant *W. chinensis* is called as Kesaraja in Ayurveda and Potrilaiikaiyan and Potrilaiikaiyanthagarai in Siddha System of Medicine and also has medicinal value in traditional Chinese medicine and Unani.^[4] As per the Ayurvedic Pharmacopoeia of India, the whole plant has been used for various ailments such as piles, diarrhea, alopecia, helminthiasis, jaundice, cough, headache, gynecological disorder and ulcer,^[5] whereas in Siddha Pharmacopoeia of India, the same plant has been used for night blindness and ulcer.^[6]

It is generally considered that *W. chinensis* is native to India, China, and South-East Asia, whereas *W. trilobata* is a different species that originates from Caribbean, Central America, and north of South America and was introduced to Asia as an ornamental plant; being highly probable, it escaped cultivation and got naturalized.^[7] *W. trilobata*, as its name indicates, has distinct three lobes on its leaves, whereas *W. chinensis* has leaves with more smooth margins, rarely serrated or lobed. Most often, *W. trilobata* was used in the place of *W. chinensis* because of its ubiquitous availability.

Most of the edible plant's phytoconstituents possess free radical scavenging ability. Normally, the reactive oxygen species (ROS) generated during physiological process will be cleared by the presence of antioxidants in the body. However, owing to inadequate antioxidant

defense, this balance will be disturbed, favoring the ROS increase that end up in oxidative stress, which leads to several disorders.^[8] Abundant use of acetaminophen (AAP) for pyrexia especially fevers of viral entity often ended up with toxicity. The mechanisms of AAP-induced liver injury are highly complex, and many intracellular and extracellular events are involved in this pathophysiological process, including metabolism of AAP to its metabolite N-acetyl-p-benzoquinone imine (NAPQI), mitochondrial oxidative stress, ER stress, autophagy, sterile inflammation, and microcirculatory dysfunction.^[9] Hence, the key proteins involved in the individual process were selected for the docking study with wedelolactone, a marker compound for *E. prostrata*, and *W. chinensis*, and both plants possess hepatoprotective potential.^[10,11] The selected targets (PDB ID)^[12] are peroxisome proliferator activated receptor- α (PPAR- α : 3KDU), AMP-activated kinase (AMPK: 6C9F), c-Jun N-terminal kinase-1 (JNK-1: 3ELJ), epidermal growth factor receptor (EGFR: 2RGP), nuclear factor erythroid 2-related factor-2 (Nrf2: 2FLU), alanine transaminase (ALT: 3IHJ), alkaline phosphatase (ALP: 1ZEB), gamma glutamyl transpeptidase (GGT: 4GDY), cartesenoide-activated receptor (CAR: 1XNX), frizzled receptor (4F0A), farnesoid X receptor (FXR: 5Q0I), extracellular signal regulated kinase 1 (ERK1: 2ZOQ), liver X receptor-alpha (LXR: 1UHL), mitochondrial glutamate dehydrogenase (GDH: 1L1FA), p53 (1C26), mammalian target of rapamycin complex 1 (mTORC1: 5H64), cytochrome P450 1A2 (CYP1A2: 2HI4), cytochrome P450 2E1 (CYP2E1: 3E6I), 5-lipoxygenase (5-LO: 308Y), thrombin (2A2X), uncoupling protein 2 (UCP-2: 2LCK), glycogen synthase kinase (GSK-1: 1GNG), retinoid X receptor (RXR: 4K4J), nuclear factor-kappa B (NF- κ B: 1SVC), and pregnane X receptor (PXR: 2QNV).^[13] Hence, the present study aimed to characterize the plants, test their antioxidant and free radical scavenging ability, and explore *in silico* hepatoprotective potential against acetaminophen-induced liver damage.

MATERIALS AND METHODS

Plant materials

Three plant species in Asteraceae family, namely *Wedelia trilobata* (Osbeck) Merr. Philipp J. (syn. of *Solidago chinensis* Osbeck; *Wedelia calendulacea* Less), *W. trilobata* (L.) Hitchc. (syn. of *Sphagneticola trilobata* L.), and *Eclipta prostrata* (L.) L. (syn. *Eclipta alba* L.) were collected from Chennai and nearby areas and taxonomically identified at CSMRADDI (CCRAS), Arumbakkam, Chennai, and its voucher specimens (*W. chinensis* [00473], *W. trilobata* [00626], and *E. prostrata* [00530]) were preserved in the Department of Botany, CSMRADDI, Chennai. The plants were subjected to botanical testing by

macro-morphological, micro-morphological, and powder microscopical characters. Plant powders were treated with benzene, chloroform, ethyl acetate, methanol, acetone, ethanol, and water for fluorescence characters under ultraviolet (UV) light of 366 nm.^[14]

Extraction

All the three plants were collected, shade dried, powdered, and extracted with ethanol (80°C) for 48 h under reflux by Soxhlet extraction. It was filtered and concentrated under reduced pressure, made free of solvent to obtain a semisolid mass. The preliminary phytochemical screening of *W. chinensis*, *W. trilobata*, and *E. prostrata* was determined.^[15]

High-performance thin-layer chromatography fingerprinting of *Wedelia chinensis*, *Wedelia trilobata*, and *Eclipta prostrata* extracts

Powders of *W. chinensis*, *W. trilobata*, and *E. prostrata* (4 g) were extracted with 40 ml of ethanol (80°C) under reflux for 8 h. The extracts were concentrated to 10 ml solution. Different volumes of these solutions were applied on a precoated silica gel 60 F₂₅₄ of 2 mm thickness aluminum plates to a bandwidth of 6 mm using CAMAG HPTLC system equipped with TLC Linomat IV applicator and TLC scanner 3, and win CATS 1.4.4. Software (Camag, Muttenz, Switzerland) was used for HPTLC analysis. The plate was developed in a solvent system of toluene:ethyl acetate:formic acid (7:2.5:0.5) up to 80 mm. The developed plates were visualized and scanned under UV 254 nm (D2 lamp) and 366 nm (Hg lamp) and under white light at 520 nm (tungsten W lamp) after derivatization in vanillin-sulfuric acid spray reagent. R_f values of the spots were recorded.^[16]

In vitro antioxidant activity

Determination of diphenyl picrazyl hydrazide radical scavenging activity

To 1 ml of ethanolic extracts of the three plants at various concentrations, 1 ml of 10 μM DPPH was added and incubated at 37°C for 30 min. Change in the absorbance of reaction mixture was read at 517 nm in an UV-visible spectrophotometer.^[17] The percentage radical scavenging activity was calculated by the following formula:

$$\% \text{inhibition} = \frac{(\text{Absorbance of control} - \text{Absorbance of test})}{(\text{Absorbance of control})} \times 100$$

Determination of iron chelating activity

A volume of 0.1 ml of 2.0 mM ferrous chloride was added to 1.0 ml of ethanolic extracts of the three plants at different concentrations. After vortexing, the mixture was incubated for about 10 min and the reaction was initiated by the addition of 0.4 ml of 5 mM ferrozine solution. The mixture was vigorously shaken and left to stand for 10 min at room temperature. The absorbance of ferrozine-Fe²⁺ complex formation was measured at 562 nm in the UV-visible spectrophotometer.^[17] The percentage inhibition was calculated as follows:

$$\frac{(\text{Absorbance of control} - \text{Absorbance of test})}{(\text{Absorbance of control})} \times 100$$

In silico screening

Drug-likeness analysis

The marker compound, wedelolactone, was subjected to predict the drug-likeness properties as per Lipinski's rule of five (Ro5). Lipinski's screening was performed using Molinspiration web server,^[18] and the physicochemical properties of ligand were calculated.

Docking analysis

Wedelolactone was subjected to docking studies with acetaminophen target proteins using Autodock 4.2 (Molecular Graphics Laboratory (aka Olson Laboratory), U.S.A), and binding energies were calculated. Further, wedelolactone was subjected to ADMET prediction for pharmacokinetics and pharmacodynamics properties.

Structure retrieval

The three-dimensional crystal structures of the target proteins were retrieved from the Protein Data Bank. The ligand molecule, wedelolactone, was retrieved from Pub Chem server^[19] and was refined using ACD Chem Sketch software (Advanced Chemistry Development, Canada), a tool that offers functionalities such as structure refining and optimization.

Docking studies

The target proteins were docked with wedelolactone using Auto Dock 4.2. The free energy of binding between the ligand and proteins was calculated. Auto Dock 4.2. uses charge-based desolvation force fields and well-defined improved models of the unbound state. The docking analysis attempts to bind the ligand to the obtained binding sites of the target protein and produces the best docked conformations with minimal energy, as the output. A semi-flexible docking protocol was applied, wherein the target proteins were kept rigid, while the phytochemical ligand was kept flexible for being docked upon. A 5Å° grid was built surrounding the binding pocket. Grid map dimensions were set to yield the receptor model that included atoms within 0.5Å° of the grid center. All the other parameters were kept at default, and Lamarckian genetic algorithm was chosen to predict the best conformers. The protein-ligand complexes were viewed using Molegroviewer software (Molegro Molecular Viewer, CLC bio company, Denmark). Each protein consists one or more chains; the active sites were predicted based on their ligands which were previously docked; if not, each chain of the protein was individually docked and the chain which has less binding energy with ligand was reported.

Absorption, Distribution, Metabolism, Elimination, and Toxicity studies

The molecular structure of ligand was submitted to ADMET-SAR web tool^[20] to examine their drug likeliness and different pharmacokinetic and pharmacodynamic parameters including human intestinal absorption (HIA); Caco-2 permeability; aqueous solubility; blood-brain barrier penetration; renal organic cation transportation; cytochrome P (CYP) inhibitory promiscuity; cytochrome P450 inhibition; AMES toxicity; fish toxicity; rat acute toxicity; *Tetrahymena pyriformis* toxicity; human ether-ago-go-related gene inhibition; and mutagenic, tumorigenic, and reproductive risks.^[9]

RESULTS

Pharmacognostic characterization of the herbs

Macro-morphology of the plants

Comparative macro-morphology of the three plants is depicted in Figure 1.

Wedelia chinensis

Stem cylindrical, branched with pubescence at surface, small roots at the lower nodes. Leaf 2.7 to 7.5 cm long and about 1.8 to 2.5 cm wide. Leaves opposite, sub-sessile, and lanceolate to oblong in shape. Margin entire, sparsely mucronulate-serrulate, base tapering. Apex acute, scabrous, covered with short, white trichomes. Flower had a solitary head, slender with tetragonous rayed flower yellow in color, in axillary or at the terminal heads.

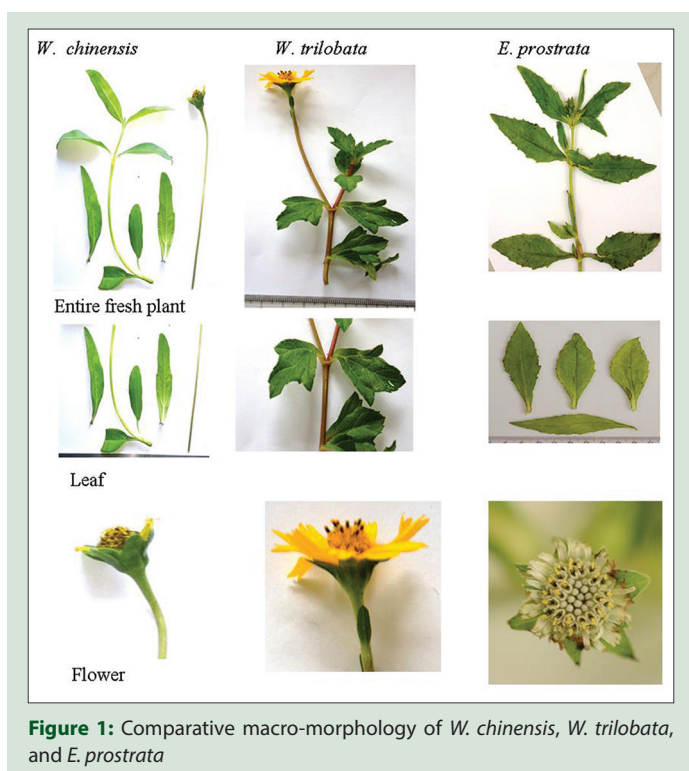


Figure 1: Comparative macro-morphology of *W. chinensis*, *W. trilobata*, and *E. prostrata*

Wedelia trilobata

Stem decumbent, branched and cylindrical in shape, with nodes bearing roots which had lateral or secondary branched small hairs. Leaf three lobed with a serrated margin had small petioles. Flower solitary, yellow in color with slender and long peduncles.

Eclipta prostrata

Stem erect and cylindrical; pubescence at the surface and branched with distinct nodes and internodes. Leaf 2–9 cm long and about 1–2.5 cm wide, opposite, sub-sessile to sessile, lanceolate to oblong in shape, dentate margin, acute apex and pubescence surface. Lower surface paler. Flower solitary with tubular disc-rayed flower white in color.

Micro-morphology

Comparative micro-morphology of the three plants is given in Figure 2.

Wedelia chinensis

In stem, epidermis had a thin-layered cuticle covered with three-celled unicellular trichomes and glandular trichomes with eight-celled heads. Hypodermis had 3–5 rows of walled polygonal collenchymatous cells yellow in color. Cortex composed of aerenchyma with certain large intracellular space. Endodermis and pericycle layer were distinct. Leaf dorsiventral, covered with a prominent cuticle had thin-walled epidermis in the upper and lower surfaces. Palisade cells were present in a single layer on the upper surface. It consisted of well-developed spongy parenchyma and amphicribal vascular bundles situated at the center surrounded by a thick-walled bundle sheath. Palisade ratio was about 3–4 and the stomatal index was 12–14 on the upper surface and 22–25 on the lower surface.

Wedelia trilobata

In stem, epidermis covered with a thin-layered cuticle, glandular trichomes with eight-celled heads and unicellular trichomes with three-celled wide heads. The hypodermis consisted of thin-walled polygonal collenchymatous cells. Cortex consisted of aerenchyma cells with large

intercellular spaces. Endodermis and pericycle layer were distinct. Leaf was dorsiventral. Epidermis showed a prominent cuticle. It had lower and upper epidermis and a single layer of palisade cells on upper epidermis. It also consisted of well-developed spongy parenchyma and amphicribal vascular bundles were present at the center surrounded by thick-walled bundle sheath. The palisade ratio was about 3–5 and the stomatal index was 3–5 for the upper surface and 18–22 for the lower surface.

Eclipta prostrata

Upper epidermis had thin-walled rectangular cells covered with a thick cuticle. Hypodermis had eight rows of collenchymatous cells. Cortex had thin-walled parenchymatous cells embedded with air cavities followed by a single layer of endodermis. Endodermis had central stellar region with collateral wedge discontinuous ring of vascular bundles capped with lignified pericyclic fibers combined with narrow intra fascicular parenchyma cells. Vascular bundles composed of usual elements. Pith had thin-walled parenchymatous cells with a few prismatic calcium oxalate crystals. In leaf, epidermis composed of a layer covered with warty, tubercle, pointed stiff uniseriate trichome followed by a single layer of palisade layer. Hypodermis had thin-walled polygonal collenchymatous layer of about 2–5 cells. Central region had five bicollateral vascular bundles of usual elements. The lamina was dorsiventral. Mesophyll differentiated into palisade and spongy parenchyma cells. Epidermis composed of a single layer of palisade cells with warty, tubercle, pointed stiff uniseriate trichomes. Endodermis consisted of spongy parenchyma cells of about seven layers transversed with fibrovascular strands with a few oil globules and a few prismatic calcium oxalate crystals. Palisade ratio 3.2–4.5 and the stomatal index 18–20.5 for the upper surface and 24–27.3 for the lower surface.

Powder microscopy

Comparative powder microscopy of the three plants is given in Figure 3.

Wedelia chinensis

In powder microscopy, *W. chinensis* appeared greenish brown. Trichomes were long, straight, or bent multiserial had basal cells. Stomata anisocytic type at the upper and lower epidermis on surface view. Mesophyll had cluster and prismatic calcium oxalate crystals embedded in the parenchyma cells. Lamina had fragments of laminar layer with a single layer of epidermal cells covered with thin sinuous cuticle and a single palisade layer of spongy parenchyma cells. Vessel elements were annular type associated with spiral and laticiferous cells. Fibers were long with narrow lumen. Cicatrix type of cells were present at the lower base of trichomes.

Wedelia trilobata

W. trilobata was greenish brown. The trichomes had two-celled cicatrix pointed trichomes. The tracheids were thick walled. The lamina had a single layer of palisade cells at the epidermis.

Eclipta prostrata

Stomata was anisocytic/anamocytic stomata embedded at the surface of the epidermal layers. Vessel elements were spiral, spongy parenchyma cells and mesophyll cells embedded with a few prismatic calcium oxalate crystals and oil globules.

Fluorescence characters

The results of fluorescence characters are presented in Figure 4. *W. chinensis* appeared red, red, red, pink, creamy pink, creamy pink, and no fluorescence with different solvents namely benzene, chloroform, ethyl acetate, acetone, methanol, Ethanol and water, respectively. With the same solvent, *W. trilobata* assume red, red, red, red, red, red, and no

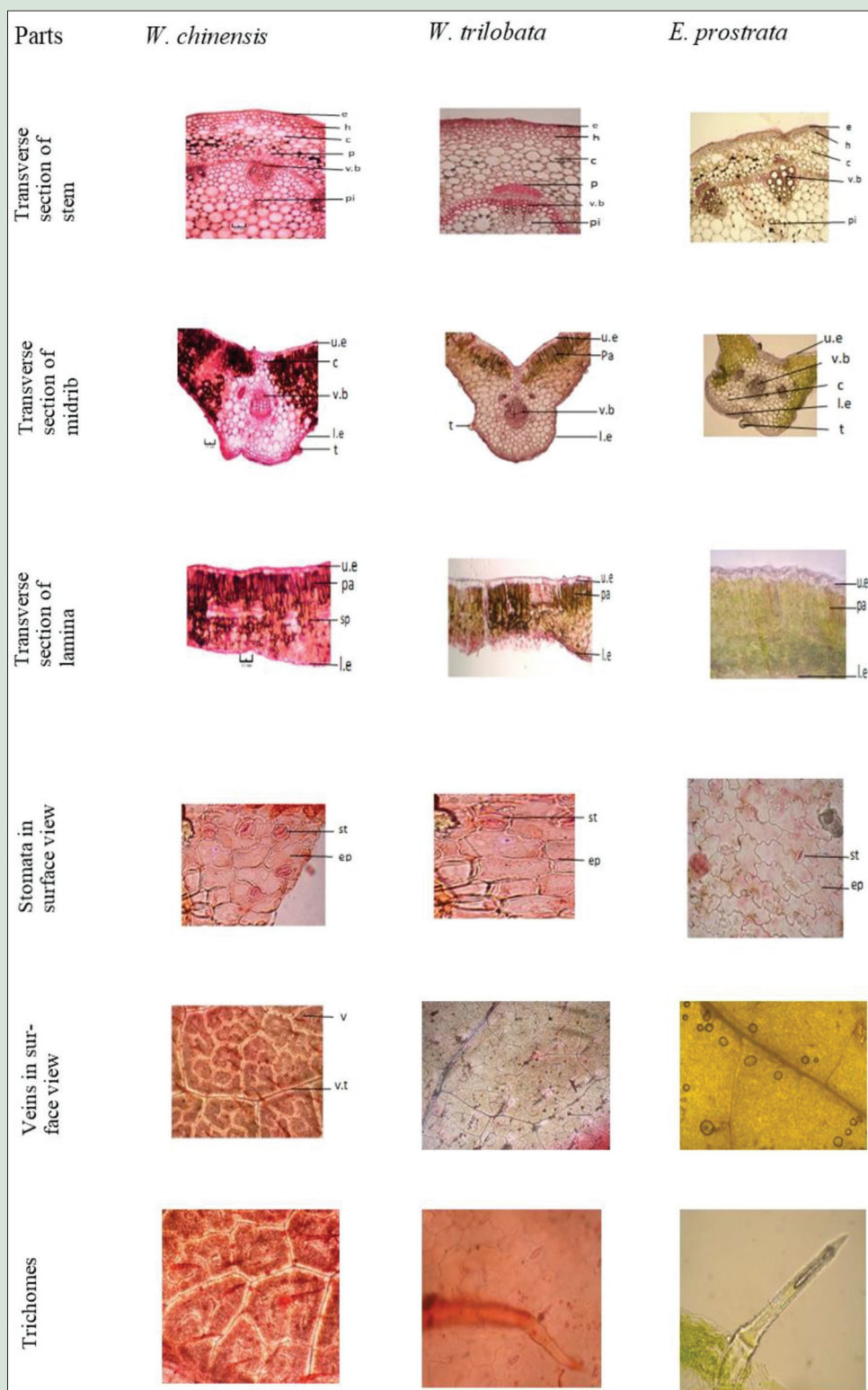


Figure 2: (a) Comparative micro-morphology of stem midrib, lamina, stomata, veins and trichomes of *W. chinensis*, *W. trilobata*, and *E. prostrata*. e/ep: Epidermis; p: Parenchyma; u.e: Upper epidermis; st: Stomata; h: Hypodermis; v.b: Vascular bundles; l.e: Lower epidermis; pa: Palisade cells; c: Cortex; pi: Pith; t: Trichome; v: Vein; v.t: Vein terminal

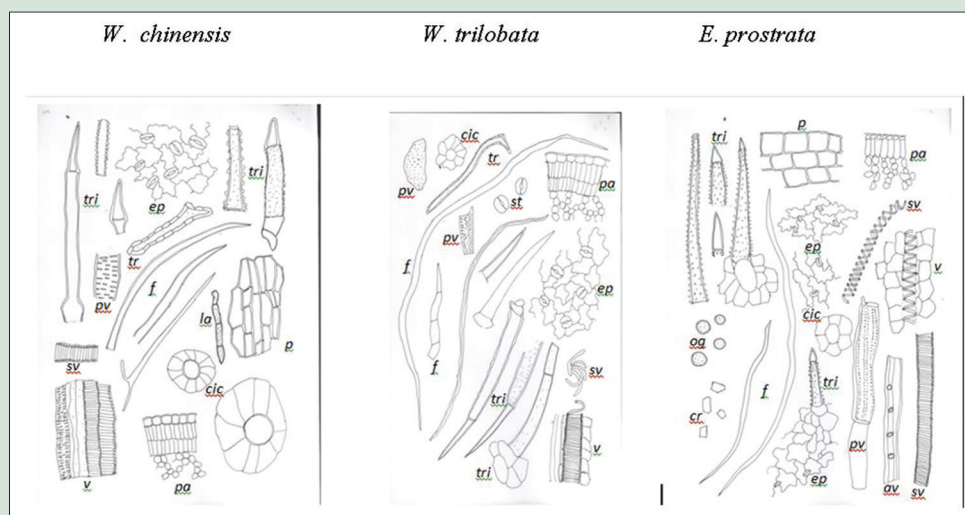


Figure 3: Comparative powder microscopical study of *W. chinensis*, *W. trilobata* and *E. prostrata*. tri: Trichomes; pv: Pitted vessel; sv: Spiral vessels; f: Fibres; pa: Parenchyma; cic: Cicatrix; tr: Tracheids; st: Stomata; pv: Pitted vessel; ep: Epidermis; og: Oil globules; cr: Crystals of calcium oxalate; av: Annular vessels; p: Parenchyma; v: Vessel

fluorescence, respectively. In case of *E. prostrata*, with the same solvent, the powder assumed no fluorescent, light blue, bluish pink, pink, bluish white, bluish white and green, respectively.

Preliminary phytochemical screening

The alcoholic extracts of three species were subjected to qualitative phytochemical analysis. In preliminary phytochemical screening, *W. chinensis* revealed the presence of phenol, steroids, tannin, flavonoids, and coumarins. *E. prostrata* revealed the presence of phenol, cardiac glycosides, coumarin, tannin, saponin, and flavonoids. *W. trilobata* revealed the presence of phenol, steroids, glycosides, tannin, saponin, and flavonoids.

High-performance thin-layer chromatography fingerprinting profile

The result of the HPTLC analysis is given in Figure 5.

HPTLC analysis with specific solvent system of Toluene:ethyl acetate:formic acid (7:2.5:0.5) revealed 12 and 12 spots at various R_f when viewed under UV 254 nm and 366 nm, respectively. After derivatization, 13 spots were observed. Whereas *W. trilobata* revealed 10 and 7 spots at various R_f when viewed under UV 254 nm and 366 nm, respectively. Thirteen spots were observed after derivatization. The marker compound wedelolactone was visible in 254 nm and 366 nm but not visible after derivatization of the plate with vanillin-sulfuric acid reagent. The compound wedelolactone was present in *W. chinensis* and not in *W. trilobata*. Because wedelolactone is a marker for *E. prostrata*, all the three plants were subjected to HPTLC fingerprinting and their chemical profiles were compared, which is represented in Figure 6.

Evaluation of antioxidant potential

The liver is the most frequent target organ in terms of drug toxicity. In response to oxidative stress, the production of radical species (ROS and reactive nitrogen species) increased, which induces oxidative stress including increase of cellular oxidants, lipid peroxidation and depletion of antioxidants in the liver with consequent release of marker enzymes of hepatotoxicity.^[21] Hence, the *in vitro* assay was carried out to evaluate its antioxidant potential through DPPH and iron chelating assay. In DPPH assay, IC_{50} value of *E. prostrata* was 190 $\mu\text{g/ml}$ and that of *W. chinensis* was 1.24 $\mu\text{g/ml}$, whereas that of *W. trilobata* was 1411.7 $\mu\text{g/ml}$. For the

Table 1: Drug-likeness properties of wedelolactone

Drug-likeness properties	Wedelolactone
Molecular weight	314.25
Log P	2.30
Log S	1.50
H bond acceptors	6
H bond donor	5
Rotatable bonds	1
PSA	113.27
RO5 violation	0
Refractivity	77.1457
Molar volume	247.74
Drug-likeness score	0.94

PSA: Polar surface area

Table 2: Absorption, Distribution, Metabolism, Excretion, Toxicity predicted properties of wedelolactone

Property	Wedelolactone
BBB	BBB-
HIA	HIA +
Caco-2 permeability	CaCo2-
P-glycoprotein substrate	Substrate
Renal organic cation transporter	Noninhibitor
Subcellular localization	Mitochondria
CYP450 2C9 substrate	Nonsubstrate
CYP450 2D6 substrate	Nonsubstrate
CYP450 3A4 substrate	Nonsubstrate
CYP450 1A2 inhibitor	Inhibitor
CYP450 2C9 inhibitor	Noninhibitor
CYP450 2D6 inhibitor	Noninhibitor
CYP450 2C19 inhibitor	Inhibitor
CYP450 3A4 inhibitor	Noninhibitor
CYP inhibitory promiscuity	Low CYP inhibitory promiscuity
AMES toxicity	Ames toxic
Carcinogens	Noncarcinogen
FHMT	High FHMT
TPT	High TPT
HBT	High HBT
Biodegradation	Not readily biodegradable
Acute oral toxicity	III
Carcinogenicity (three classes)	Not required

BBB: Blood-brain barrier; HIA: Human intestinal absorption; CYP: Cytochrome P; FHMT: Fish toxicity; TPT: Tetrahymena pyriformis toxicity; HBT: Honey bee toxicity

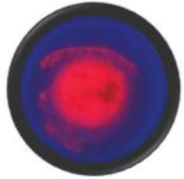
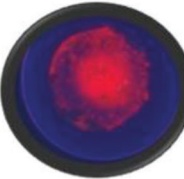
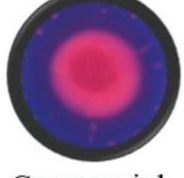
Solvents	<i>W. chinensis</i>	<i>W. trilobata</i>	<i>E. prostrata</i>
Benzene	 Red	 Red	 No fluorescence
Chloroform	 Red	 Red	 Light blue
Ethylacetate	 Red	 Red	 Bluish pink
Acetone	 Pink	 Red	 Pink
Methanol	 Creamy pink	 Red	 Bluish white
Ethanol	 Creamy pink	 Red	 Bluish white
Water	 No fluorescence	 No fluorescence	 Green

Figure 4: Fluorescence characters observed under ultraviolet light of *W. chinensis*, *W. trilobata*, and *E. prostrata*

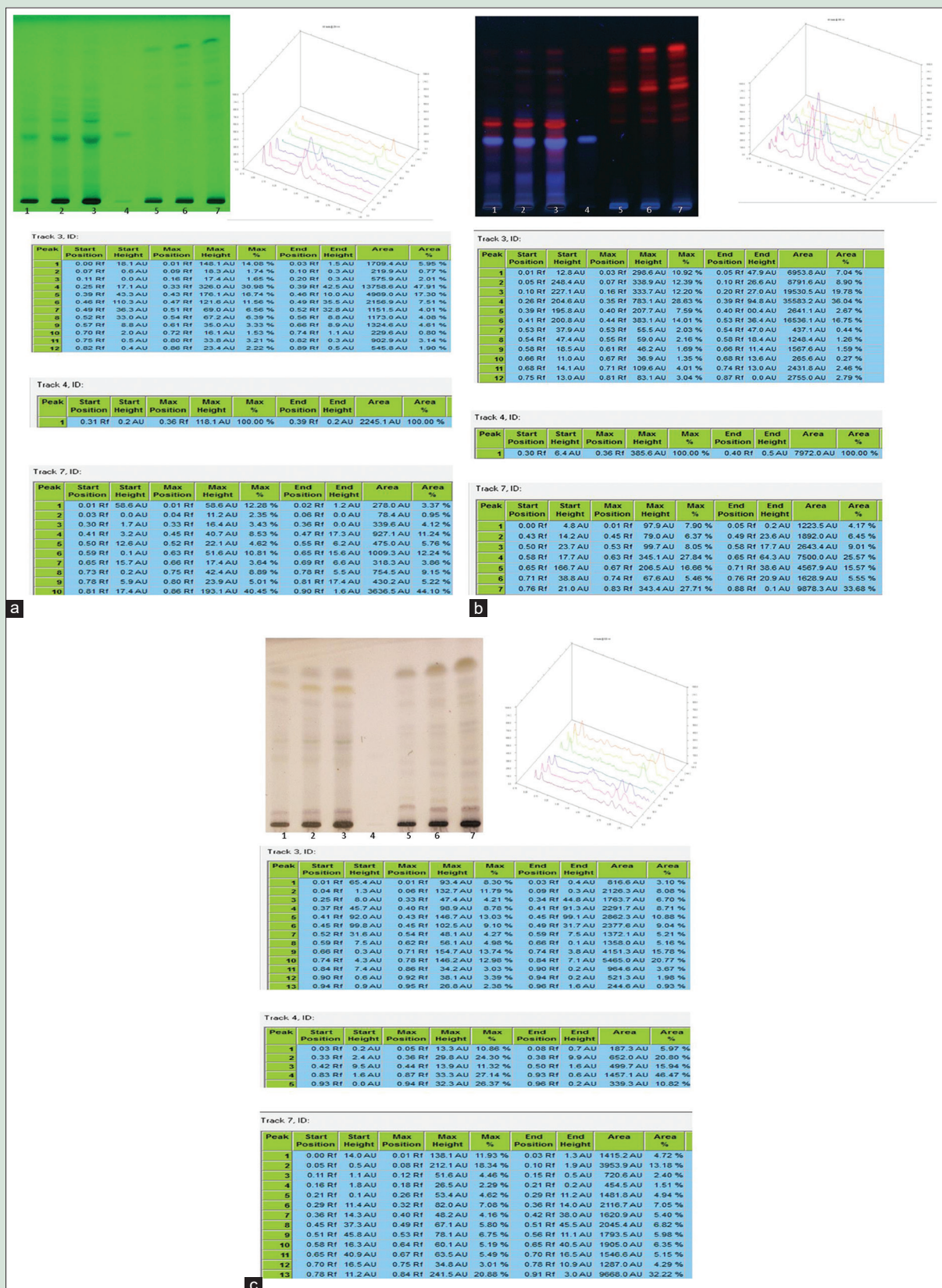


Figure 5: (a) High-performance thin-layer chromatography fingerprinting profile of *W. chinensis* (track 1: 5 µl, track 2: 10 µl; track 3: 15 µl) and *W. trilobata* (track 5: 5 µl, track 6: 10 µl; track 7: 15 µl) with marker wedelolactone (Track 4: 5 µl) under (a) 254 nm, 366 nm and 520 nm

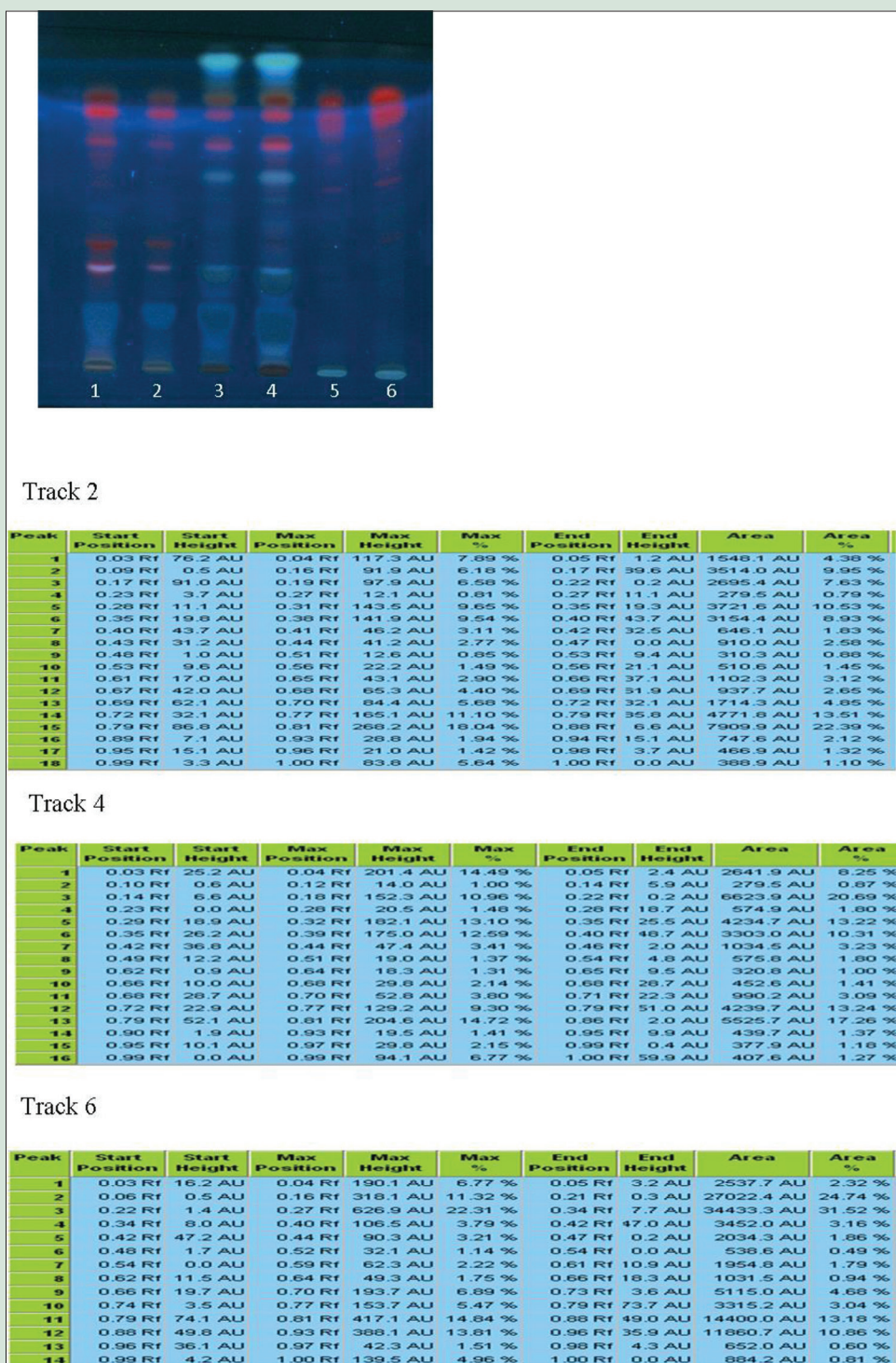


Figure 6: Comparative high-performance thin-layer chromatography fingerprinting profile of *W. chinensis* (track 1: 5 μ l, track 2: 10 μ l), *E. prostrata* (track 3: 5 μ l, track 4: 10 μ l) and *W. trilobata* (track 5: 5 μ l, track 6: 10 μ l) under 366 nm

reference drug quercetin, IC_{50} was 11.87 μ g/ml. In iron chelating activity assay, the IC_{50} value of *E. prostrata* was 340 μ g/ml and that of *W. chinensis* was 755.555 μ g/ml, whereas that of *W. trilobata* was 2,892 μ g/ml. For the reference drug, sodium ethylene diamine tetra acetic acid, IC_{50} was 10 μ g/ml.

In silico studies

Studies are available stating that both *W. chinensis*^[22] and *E. prostrata*^[23]

possess hepatoprotective activity and contain a common marker wedelolactone. It was proved that the wedelolactone has hepatoprotective activity in CCl_4 and concanavallin A-induced liver injury.^[24] The biological mechanism of these plants on hepatoprotection remains elusive. Hence, the *in silico* studies were carried out to predict the role of wedelolactone in acetaminophen-induced hepatotoxicity. The drug likeliness and pharmacokinetics of wedelolactone were predicted, which are represented in Tables 1 and 2.

Table 3: Binding energy, interacting residues and hydrogen bond interactions of Wedelolactone with selected target proteins

S.no	Target protein	Binding energy	Interacting residues	Hydrogen bond Interactions
A.	PPAR- α	-9.25	Leu 344,Phe 361, Met 366, Cys 278, Tyr314,Ser 230, Tyr 484,	Cys 278, Tyr314, Ser 230, Tyr 484
B.	AMPK	-8.21	Gly161,Asp159, Phe160, Ala158, Ile79, Leu148, Glu96, Val96, Tyr97, Leu24, Val32,Lys47	Ala158, Val 98
C.	JNK-1	-7.86	Ala 36, Ala53, Arg69, Asn156, Gln37, Glu109, Gly33,Gly35,Gly38,ile 32, ile 86,leu 110, leu 168, Lys55, Met 111, Ser 34, Val 40, Val 158	Met111,Ala36, Lys 55, Glu109
D.	EGFR	-7.12	Leu 792, Met 1062, Gln 791, Met 793, Leu 844, Gly 736, Thr 854,Leu 718, Thr 790, Ala 743, Asp855	Met 793,Thr 854, Asp 855
E.	Nrf2	-8.23	Ile 559, Thr 560, Val 514, Cys 513, Val 512, Val 465, Leu 365, Ile 416, Ala 366, Val 604	Ile 559, Val 514, Val 465, Leu 365
F.	ALP	-6.80	Ile 278, Tyr 325, Glu 277,Arg 280	Arg 280,Tyr 325
G.	ALT	-5.8	Tyr 302,Gly342,Met439,Asn 94, Lys341	Tyr 302, Gly 342
H.	GGT	-6.5	Val 43,Tyr 38, Arg 55,Lys 48, Ser 51, Ala 45	Val 43, Arg 55, Ala 45
I.	CAR	-6.8	Lys 235, Met 236, Phe 227, His 213, Leu 216, Asn 175, Leu 212, Ile 174,Phe 171	Phe 171, Asn 175
J.	Frizzled receptor	-7.3	Tyr 57, Ala 60, Trp 61, Trp 286, Gln 58, Glu 62, Lys210	Glu 62, Trp 61
K.	FXR	-7.42	Trp 458, Leu 291, Tyr 373, Ser 336, Phe 333, Trp 473, Met 332, Val 329	Ser 336, Trp 473
L.	ERK 1	-7.38	Asp 184, Val 56, Gly 51, Lys 131, Met 125, Glu 126	Asp 184, Met 125, Lys 131
M.	LXR	-7.11	Phe 257, His 421, Trp 443, Ile 295, Thr 302, Leu 299	Thr 302, Trp 443
N.	GDH	-7.79	Thr 483, Arg 482, Arg23, Leu 365, Lys 362, Asp 480, Asp 361, Leu 479, Ile 369, Val 371	Leu 479
O.	p53	-5.58	Glu 326, Gly 325, Glu 349, Asn 345	Glu 326, Glu 349, Asn 345
P.	mTORC1	-7.46	Trp 274, Leu 224, Leu 318, Leu 48, Ala 47, Cys 317	Trp 274, Leu 318, Leu 48
Q.	CYP1A2	-6.51	Met 448, Leu 450, Phe 451, Gly 452, Arg 457, Glu 446, Lys 442, Ile 440, Lys 465	Met 448, Leu 450, Phe 451, Lys 465
R.	CYP2E1	-8.17	Arg 484, Asp 470, Ile 469, Lys 486, Leu 463	Arg 484, Asp 470, Lys 486, Leu 463
S.	5- lipoxygenase	-7.67	Leu 230, Tyr 234, Tyr 467, Ile 320, Lys 319, Gln 656, Glu 228, Met 231	Leu 230, Lys 319, Gln 656, Glu 228
T.	Thrombin	-7.50	Asp 189, Gly219, Gly226, Phe227, Ser 195, Glu192,Cys220	Asp 189, Glu 192
U.	UCP-2	-7.56	Arg 143, Gln 147, Glu 170, Ile 166, Thr 159,Val 140, Ala 162	Arg 143, Thr 159
V.	GSK-1	-6.58	Leu 132, Val 10, Asp 200,Val 135, Tyr 134, Ile 62	Asp 200,Val 135,Tyr 134, Ile 62
W.	PXR	- 6.86	Tyr 328,Leu 319, Leu 32, Leu 318, Leu 209, Glu 309	Leu 209, Glu 309
X.	RXR	-7.01	Trp 305, Asn 306, Leu 433, Cys432, Leu 436, Ile 268, Phe 313, Ala 327, Leu 326, Gln 275	Ala 327
Y.	NF- κ B	-6.82	Asn139, Gly 68,Lys 117, Pro 55, Val 115, Ile 142, Arg 59,Leu 143, Arg 57, Gly 141	Asn139, Ile 142, Arg 59, Leu 143

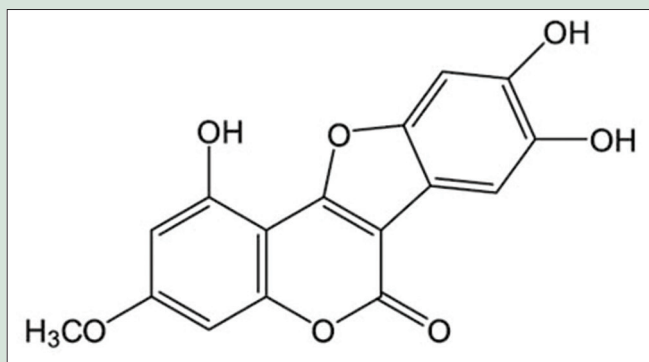


Figure 7: Structure of wedelolactone: molecular formula: $C_{16}H_{10}O_7$, IUPAC name: 1, 8, 9-trihydroxy-3-methoxy-6H-[1]benzofuro[3,2-c]chromen-6-one

The key protein targets involved in acetaminophen toxicity were selected and docked with the marker compound, wedelolactone [Figure 7] whose binding energy (docking score), interacting residues, and hydrogen bond interactions are tabulated in Table 3.

It is considered that, the lesser the G score (binding energy) value, greater is the binding of the ligand with the protein. Those target proteins, which have binding energy of -6 and below with wedelolactone were considered as probable targets for wedelolactone. From the G score values, it is observed that wedelolactone showed lesser G score value, i.e., high affinity toward target proteins in the following order: PPAR- α , AMPK, Nrf2, CYP2E1, EGFR, JNK1, UCP-2, thrombin, 5-lipoxygenase, mTORC1, RXR, FXR, LXR, frizzled receptor, GDH and Erk-1. Hydrogen bond interactions of wedelolactone at the active site of target proteins were observed, which influence high binding affinity toward the protein. The molecular representation of docking proteins with wedelolactone are depicted in Figure 8a-c.



Figure 8a: Molecular representation of docking proteins with docked compound. Conformation of wedelolactone shown by sticks inside the binding pocket of PPAR- α (A), AMPK (B), JNK-1 (C), EGFR (D), Nrf2 (E), ALT (F), ALP (G), GGT (H), CAR (I), and frizzled receptor (J). The conformation of wedelolactone shown by sticks inside the binding pocket of target proteins

DISCUSSION

Pharmacognostical studies revealed that the three plants were entirely different by macro-morphology, micro-morphology, and by powder microscopy. Fluorescence characters with the different solvents were also different from each other except the marker compound wedelolactone which is present both in *W. chinensis* and *E. prostrata*, not in *W. trilobata*. This was supported by HPTLC fingerprinting profile of the plants. In comparative fluorescence study, red color was common for both *W. chinensis* and *W. trilobata*, but not in *E. prostrata*. Bluish white was observed in *E. prostrata*, but in *W. chinensis*, pink and bluish white were mixed together forms a creamy pink color. The same was observed with HPTLC fingerprinting profile, where the marker compound wedelolactone appeared bluish white fluorescent band in *E. prostrata*. The

same wedelolactone was observed in *W. chinensis*; some pink color bands were very nearer to wedelolactone making it creamy pink. However, low polar blue color-emitting other compounds were also observed in HPTLC fingerprinting of *E. prostrata*. The preliminary phytochemical screening also revealed the presence of various major groups of phytoconstituents. Reports stated that the following compounds were present in *W. chinensis*: α -pinene (21.7%), spathulenol (20.3%) limonene (14.3%);^[25] luteolin, apigenin, and indole-3-carboxyaldehyde;^[26] wedelolactone;^[27,26] norwedelolactone;^[28] bisdesmodic-osidicoleanolic acid; bisdesmosidicoleanolic acid and β -D-glucopyranosyl-3-o-[o- β -D-xylopyranosyl-(1 \rightarrow 2)- β -D-Glucuronopyranosyl]oleanolate (IV); and β -D-glucopyranosyl 3 β -[(o- β -D-xylopyranosyl-(1 \rightarrow)-(pD-glucuronopyranosyl)]-olean-12-en-28 oate).^[29-31] In *W. trilobata*, the following compounds were reported: grandiflorenin

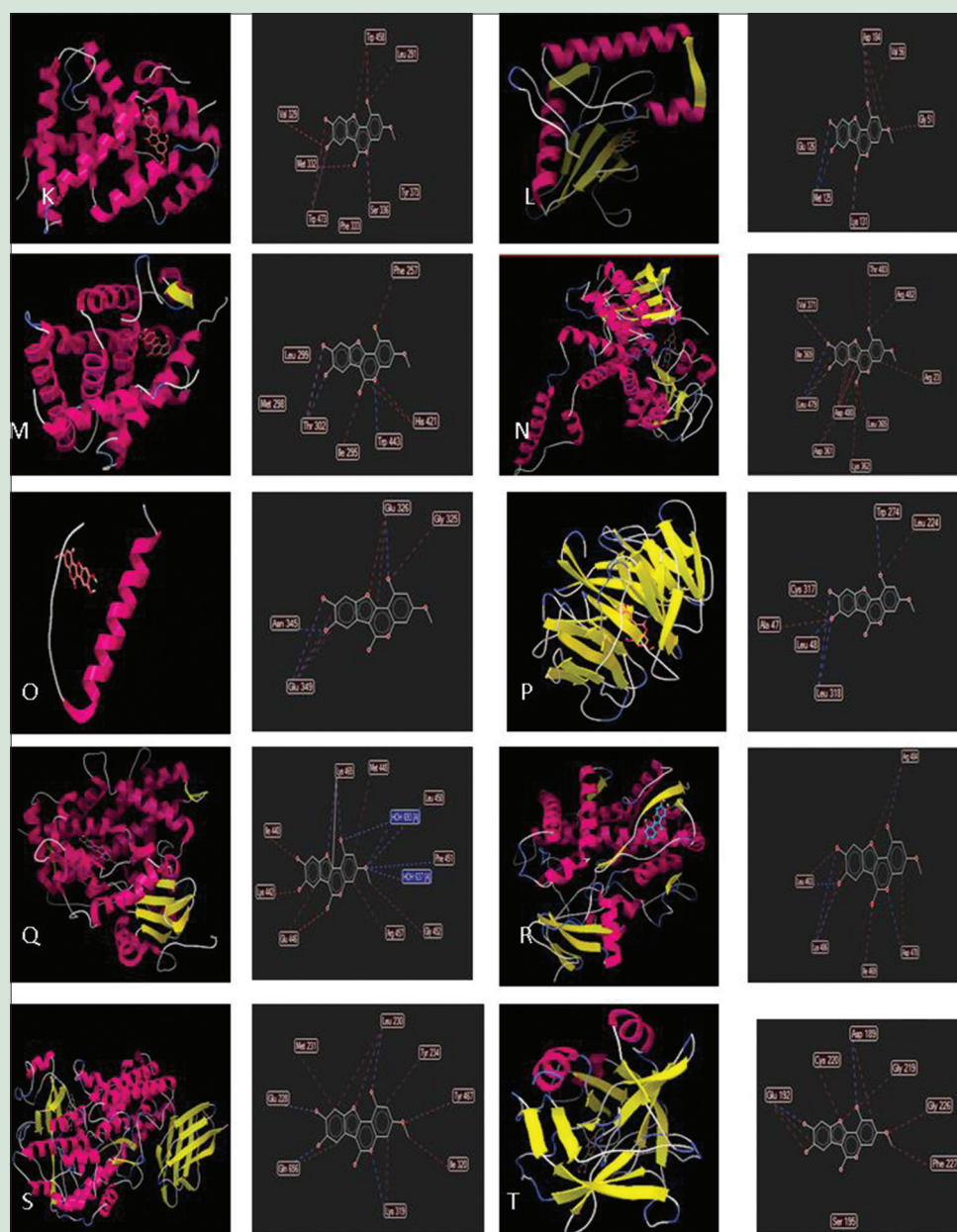


Figure 8b: Molecular representation of docking proteins with docked compound. Conformation of wedelolactone shown by sticks inside the binding pocket of FXR (K), ERK1 (L), LXR- α (M), GDH (N), p53 (O), mTOR C1 (P), CYP1A2 (Q), CYP2E1 (R), 5-lipoxygenase (S) and thrombin (T). The conformation of wedelolactone shown by sticks inside the binding pocket of target proteins

acid; 1 α -acetoxy-6 α , 9 β -dihydroxy-4, 10 α -dimethyl- 5 α H, 7 α H, 8 α H-endesm-3-en-8, 12-olide; 1 β -acetoxy-4 α -hydroxy-6 β -isobutyryloxy-9 α - isovaleryloxyprostatolide; 16 α -hydroxy-ent-kauran-19-oic acid; (3R, 4R, 6R)-3, 4-dihydroxy-1-menthene; trilobolide-6-O-isobutyrate; 1 β -acetoxy-4 α , 9 α -dihydroxy-6 β -isobutyryloxyprostatolide; 16 β , 17-dihydroxy-ent-kauran-19-oic acid; daucosterol; protocatechualdehyde, caffeic acid,^[32] and syringaresinol-4-O- β -D-glucopyranoside; pinosresinol-4-sulfate; pinosresinol-4-O- β -D-glucopyranoside; 1H-indole-3-carboxylic acid; 1H-indole-3-carbaldehyde; 2,6-dimethoxy-4-hydroxyphenol-1-O- β -D-glucopyranoside; 3,5-dimethoxy-4-hydroxyphenol-1-O- β -D-glucopyranoside,^[33] germacrene D; α -phellandrene; α -pinene; *E*-caryophyllene; bicyclogermacrene; limonene α -humulene;^[34] 3 α -Angeloyloxy-16 α -hydroxy-ent-kauran-19-oic acid; 3 α -Angeloyloxy-16 α ,17-dihydroxy-ent-kauran-19-oic acid;

3 α -Tigloyloxy-16 α -hydroxy-ent-kauran-19-oic acid; 3 α -Tigloyloxy-16 α ,17-dihydroxy-ent-kauran-19-oic acid; 3 α -Dihydrocinnamoyloxy-ent-kaur-16-en-19-oic acid; 3 α -Cinnamoyloxy-ent-kaura-9 (11), 16-dien-19-oic acid and 3 α -Cinnamoyloxy-9 β , 17-dihydroxy-ent-kaur-15-en-19-oic acid.^[35] In *E. prostrata*, the following compounds were reported: wedelolactone, demethyl wedelolactone, demethyl wedelolactone 7-o-glucoside, apigenin, luteolin, luteolin-O-glucoside, eclalbasaponins I-X, eclalbatin, ursolic acid, oleanolic acid, strychnolactone, stearic acid, lacceroic acid, 3,4, dihydroxy benzoic acid, stigmaterol, β - sitosterol, α - formylterthienyl, acetoxymethyl eneterthienyl, angeloyloxy methylene terthienyl, seneciolyxymethy leneterthienyl, tigloyloxymethyle neterthienyl, terthienyl, α -terthienyl Imethanol, 5'-isovaleryloxymethylene-2-(4-isovaleryloxybut-3-ynyl) dithiopene, 2-acetoxymethylene-5'-(but-3-en-1-ynyl) dithiopene, 2-(3'-acetoxy-4'

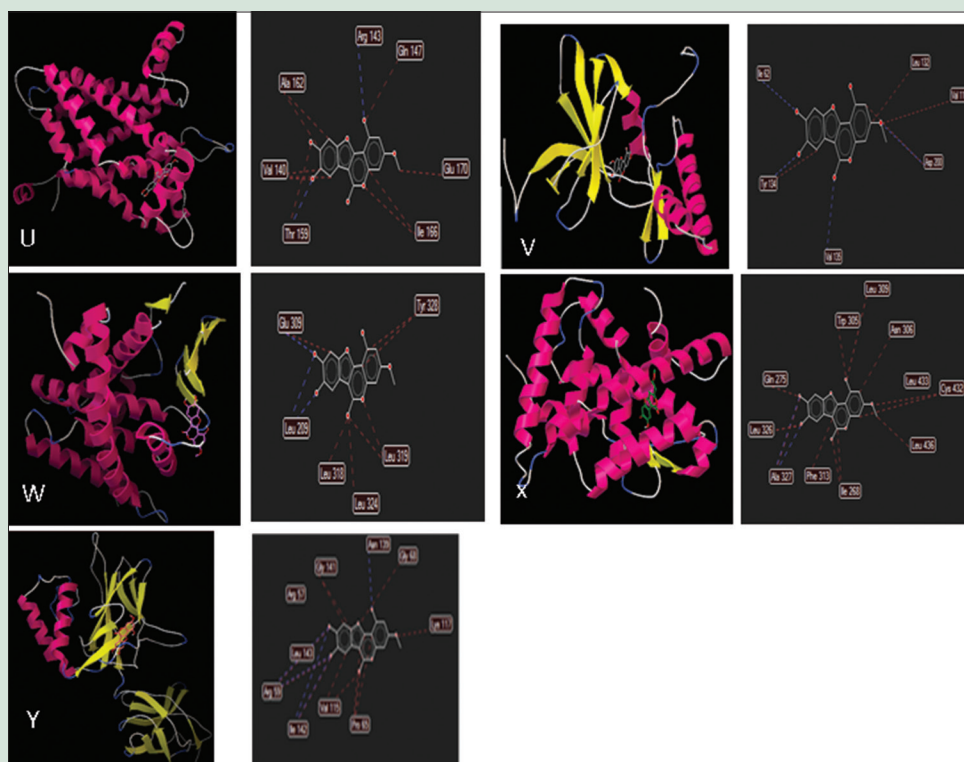


Figure 8c: Molecular representation of docking proteins with docked compound. Conformation of wedelolactone shown by sticks inside the binding pocket of UCP-2 (U), GSK1 (V), RXR (W), PXR (X), and NF- κ B (Y). The conformation of wedelolactone shown by sticks inside the binding pocket of target proteins

chlorbut-1-ynyl)-5-(pent-1,3-dienyl) thiophene, heptacosan-14-ol, hentriacontan-1-ol, nicotine, ecliptalbine, verazine, 20-epi-3-dehydroxy-3-oxo-5,6-dihydro-4,5-dehydroverazine, (20R)-4 β -hydroxyverazine, 4 β -hydroxyverazine, (20R)-25 β -hydroxyverazine and 25 β -hydroxyverazine.^[36] The methanolic extracts of the three plants were screened for antioxidant property using DPPH assay and iron chelating assay. All the three plants have antioxidant property, but the IC₅₀ was lower for *W. chinensis* in DPPH assay, which shows that *W. chinensis* has more potency than the other two plants and standard quercetin in antioxidant potential. In iron chelating activity, *E. prostrata* was found to be more potent than other two plants. The mechanism of DPPH scavenging assay is direct scavenging of radical by antioxidant.^[37] Whereas the iron chelating activity is related to Fenton's reaction where the chelator binds with the metal and thereby prevents radical formation.^[38] The difference in potency observed with *W. chinensis* and *E. prostrata* can be exploited for plant preference in specific ailments. In case of acetaminophen toxicity, the metabolite NAPQI is a radical. Hence, the radical scavenging capacity will help in the prevention and progression of injury. *In silico* screening revealed that the marker compound wedelolactone has more affinity toward the following proteins: PPAR- α , AMPK, Nrf2, CYP2E1, EGFR, JNK1, UCP-2, thrombin, 5-lipoxygenase, mTORC1, RXR, FXR, LXR, Frizzled receptor, GDH, and Erk-1. Activation of liver X receptor prevented acetaminophen-induced liver injury by induction of Phase II conjugation enzymes, especially enzymes such as glutathione transferase (GST) involved in glutathione (GSH) conjugation. It suppresses Phase I CYP2E1 enzyme which is involved in the conversion of acetaminophen into NAPQI, which forms covalent binding with sulfhydryl groups in cellular and mitochondrial proteins, results in mitochondrial oxidative stress and dysfunction, ultimately leading to hepatocyte necrosis.^[39] The nuclear receptor RXR- α is involved in the upregulation of CYP2E1. Downregulation of RXR- α will be beneficial in alleviating the APAP toxicity. Suppression of 5-lipoxygenase induces Phase II

detoxification enzyme sulfo transferase (SULT2), subsequently causing the reduction of NAPQI formation.^[40] JNK-1 amplifies mitochondrial ROS by a self-sustained activation loop, which, in turn, activates signal transduction pathway, which leads to apoptosis. Nrf2 activation induces enzymes involved in the synthesis of GSH.^[41] Activation of AMPK pathway leads to energy generation and promotes survival signaling pathway.^[13] Fatty acid β -oxidation is inhibited by acetaminophen treatment. PPAR- α encodes peroxisomal and mitochondrial enzymes, which promotes fatty acid catabolism.^[42,43] UCP-2 is a target gene of PPAR- α , which functions as an antioxidant.^[44] The inhibition of thrombin at early stage of acetaminophen toxicity may be a protective mechanism.^[45] EGFR plays a dual role both in the initiation of hepatotoxicity and subsequent regeneration in acetaminophen-induced hepatotoxicity.^[46] Frizzled receptors are involved in liver regeneration process. The FXR provides hepatoprotection by inducing the expression of several genes involved in Phase II metabolism.^[47] ERK-1 is involved in detoxification process of liver damage against oxidative stress.^[48] GDH is a mitochondrial enzyme that is involved in the metabolism of glutamate to oxoglutarate. GDH is a marker for hepatocyte damage mainly of centrilobular damage.^[49] Docking studies revealed the information about the binding of the ligand with the target and not giving the information about the outcome of an interaction. Either the interaction may be induction or inhibition, which needs to be confirmed by wet lab analysis.

CONCLUSION

From the present study, it is concluded that all the three plants are different. *W. trilobata* did not have the marker compound wedelolactone. The chemical profiling of *W. chinensis* is different from *E. prostrata*, but the marker compound is common for both. Because *W. chinensis* and *E. prostrata* were interchangeably used for common ailments, the marker compound wedelolactone might have been responsible for their shared

efficacy. *W. chinensis* was observed to be more potent antioxidant than the other two. Hence, *W. chinensis* may be a potential species for counteracting acetaminophen toxicity either as a drug or as a supportive therapy.

Acknowledgements

The authors are highly thankful to Director General, CCRAS; Director General, CCRS; Assistant Director Institute In-Charge, CSMRADDI; and Assistant Director, Institute In-Charge, SCRI for providing necessary facilities to carry out the study.

Financial support and sponsorship

Nil.

Conflicts of interest

There are no conflicts of interest.

REFERENCES

- Cooke T. The flora of the presidency of Bombay. Bot Survey India 1958;2:97-8.
- Bapalal V. Some Controversial Drugs in Indian Materia Medica. Varanasi and Delhi: Chaukambha Orientalia; 1982. p. 155-8.
- Nadkarni AK. Dr. Nadkarni's Indian materia medica. Bombay Popular Prakasam 1908;1:469-72.
- The Ayurvedic Pharmacopoeia of India. Part I. Vol. 6. New Delhi: Govt. of India, Ministry of Health and Family Welfare, Dept. of AYUSH; 2008. p. 83.
- The Ayurvedic Formulary of India. Part III. New Delhi: Govt. of India, Ministry of Health and Family Welfare, Dept. of AYUSH; 2011a. p. 440.
- The Siddha Pharmacopoeia of India. Part I. Vol. 2. New Delhi: Govt. of India, Ministry of Health and Family Welfare, Dept. of AYUSH; 2011b. p. 111.
- Invasive Species Compendium, 2019. *Sphangeticola trilobata* (*Wedelia*). Available from: <https://www.cabi.org/isc/datasheet/56714>.
- Ebrahimzadeh MA, Fereshteh P, Samira H. Antioxidant activities of Iranian corn silk. Turk J Biol 2008;32:43-9.
- Arif M, Abdul M, Muhammad UM. Molecular docking and *in silico* ADMET studies of silibinin and glycyrrhetic acid anti-inflammatory activity. Trop J Pharm Res 2017;16:67-74.
- Lu Y, Hu D, Ma S, Zhao X, Wang S, Wei G, et al. Protective effect of wedelolactone against CCl₄-induced acute liver injury in mice. Int Immunopharmacol 2016;34:44-52.
- Singh B, Saxena AK, Chandan BK, Agarwal SG, Anand KK. *In vivo* hepatoprotective activity of active fraction from ethanolic extract of *Eclipta alba* leaves. Indian J. Physiol Pharmacol 2001;45:435-41.
- Emmanuel S, Amalraj T, Ignacimuthu S. Hepatoprotective effect of coumestans isolated from the leaves of *Wedelia calendulacea* Less. in paracetamol induced liver damage. Indian J Exp Biol 2001;39:1305-7.
- RCSB PDB; 2019. p. 1-11. Available from: <https://www.rcsb.org>.
- Yan M, Huo Y, Yin S, Hu H. Mechanisms of acetaminophen-induced liver injury and its implications for therapeutic interventions. Redox Biol 2018;17:274-83.
- Shah CS, Shah NS. Pharmacognostic study of *Baliospermum montanum* Muell. Arg J Res Indian Med 1971;6:199-208.
- Harborne JB. Phytochemical Methods. London: Chapman and Hall Ltd.; 1973. p. 49-188.
- Sethi PD. High Performance thin Layer Chromatography. 1st ed., Vol. 10. New Delhi: CBS Publisher and Distributor; 1996. p. 4-28.
- Devi SA, Deepak G. Antioxidant activities of methanolic extracts of Sweet-Flag (*Acorus calamus*) leaves and rhizomes. J Herbs Spices Med Plants 2011;17: 1-11.
- Molinspiration Chemoinformatics. Calculation of Molecular Properties and Bioactivities. Available from: <https://www.molinspiration.com>.
- PubChem, NIH, US National Library of Medicine, Wedelolactone. Available from: <https://pubchem.ncbi.nlm.nih.gov/compound/Wedelolactone>.
- ADMET SAR – Laboratory Molecular Modelling and Design. Available from: <http://lmmdd.ecust.edu.cn:8000>.
- Lin SC, Lin CC, Lin YH, Shyuu SJ. Hepatoprotective effects of Taiwan folk medicine: *Wedelia chinensis* on three hepatotoxin-induced hepatotoxicity. Am J Chin Med 1994;22:155-68.
- Ahirwar DK, Saxena RC. Hepatoprotective activity of ethanolic extract of *Eclipta alba* in albino rats. Biomed Pharmacol J 2008;1:235-8.
- Luo Q, Ding J, Zhu L, Chen F, Xu L. Hepatoprotective effect of wedelolactone against concanavalin a-induced liver injury in mice. Am J Chin Med 2018;46:1-15.
- Garg SN, Gupta D, Jain SP. Volatile constituents of the aerial parts of *Wedelia chinensis* Merrill. from the north Indian plants. J Essent Oil Res 2005;17: 364-5.
- Lin FM, Chen LR, Lin EH, Ke FC, Chen HY, Tsai MJ, et al. Compounds from *Wedelia chinensis* synergistically suppress androgen activity and growth in prostate cancer cells. Carcinogenesis 2007;28:2521-9.
- Govindchari TR, Nagarajan K, Pai BR. Chemical examination of *Wedelia calendulaceae*, structure of Wedelolactone. J Chem Soc 1956;126:629-32.
- Govindachari TR, Premila MS. The benzofurannorwedelic acid from *W. calendulaceae*. Phytochemistry 1985;24:3068-9.
- The Wealth of India, Raw Materials. A Dictionary Indian Raw Materials and Industrial Products. New Delhi: Council of Scientific and Industrial Research. First Supplement Series; 2004. p. 357.
- Masoodi MH, Ahmad B, Wali AF, Zargar BA, Dar MA. Recent developments in phytochemical and pharmacological studies of *Wedelia calendulaceae*- A review. Indian J Nat Prod 2011;27:3-7.
- Wagner H, Geyer B, Kiso Y, Hikino H, Rao GS. Coumestans as the main active principles of the liver drugs *Eclipta alba* and *Wedelia calendulaceae*. PlantaMedica 1986;34:370-4.
- Wu ML, Zhang DZ, Xu QJ, Xie RR, Li QQ. Chemical constituents of *Wedelia trilobata*. Chin Tradit Herbal Drugs 2010;41:681-5.
- Ren H, Dong LM, Zhou ZY, Xu QL, Tan JW. Chemical constituents from *Sphangeticola trilobata*. Zhong Yao Cai 2015;38:1426-9.
- Silva CJ, Luiz CA, Antonio JD, Ricardo MM, Dayana F, Renata MS, et al. Chemical composition and histochemistry of *Sphangeticola trilobata* essential oil. Rev Bras Farmacogn 2012;22:482-9.
- Li SF, Ding JY, Li YT, Hao XJ, Li SL. Antimicrobial diterpenoids of *Wedelia trilobata* (L.) Hitchc. Molecules 2016;21:457.
- Quality Standards of Indian Medicinal Plants, Medicinal Plants Unit. Vol. 9. New Delhi: Indian Council of Medical Research; 2011c. p. 138-49.
- Kedare SB, Singh RP. Genesis and development of DPPH method of antioxidant assay. J Food Sci Technol 2011;48:412-22.
- Adjimani JP, Asare P. Antioxidant and free radical scavenging activity of iron chelators. Toxicol Rep 2015;2:721-8.
- Qiu Y, Benet LZ, Burlingame AL. Identification of the hepatic protein targets of reactive metabolites of acetaminophen *in vivo* in mice using two-dimensional gel electrophoresis and mass spectrometry. J Biol Chem 1998;273:17940-53.
- Pu S, Ren L, Liu Q, Kuang J, Shen J, Cheng S, et al. Loss of 5-lipoxygenase activity protects mice against paracetamol-induced liver toxicity. Br J Pharmacol 2016;173:66-76.
- Goldring CE, Neil RK, Robert EL, Randle E, Yuri NC, Williams DP, et al. Activation of hepatic Nrf2 *in vivo* by acetaminophen in CD-1 mice. Hepatology 2004;39:1267-6.
- Chen C, Hennig GE, Whiteley HE, Corton JC, Manautou JE. Peroxisome proliferator-activated receptor alpha-null mice lack resistance to acetaminophen hepatotoxicity following clofibrate exposure. Toxicol Sci 2000;57:338-44.
- Nguyen KA, Carbone JM, Silva VM, Chen C, Hennig GE, Whiteley HE, et al. The PPAR activator docosahexaenoic acid prevents acetaminophen hepatotoxicity in male CD-1 mice. J Toxicol Environ Health 1999;58:171-86.
- Patterson AD, Shah YM, Matsubara T, Krausz KW, Gonzalez FJ. Peroxisome proliferator-activated receptor alpha induction of uncoupling protein 2 protects against acetaminophen-induced liver toxicity. Hepatology 2012;56:281-90.
- Kopec AK, Joshi N, Cline-Fedewa H, Wojcicki AV, Ray JL, Sullivan BP, et al. Fibrinogen drives repair after acetaminophen-induced liver injury via leukocyte α M β 2 integrin-dependent upregulation of Mmp12. J Hepatol 2017;66:787-97.
- Bhushan B, Chavan H, Borude P, Xie Y, Du K, McGill MR, et al. Dual role of epidermal growth factor receptor in liver injury and regeneration after acetaminophen overdose in Mice. Toxicol Sci 2017;155:363-78.
- Lee FY, de Aguiar Vallim TQ, Chong HK, Zhang Y, Liu Y, Jones SA, et al. Activation of the farnesoid X receptor provides protection against acetaminophen-induced hepatic toxicity. Mol Endocrinol 2010;24:1626-36.
- Yang SY, Pyo MC, Nam MH, Lee KW. ERK/Nrf2 pathway activation by caffeic acid in Hep G2 cells alleviates its hepatocellular damage caused by t-butylhydroperoxide-induced oxidative stress. BMC Complement Altern Med 2019;19:139.
- Aullbach AD, Amuzie A. Comprehensive Guide to Toxicology in Nonclinical Drug Development, Biomarkers in Nonclinical Drug Development. 2nd ed. Academic Press, USA: Elsevier Publishers; 2017. p. 447-71.